

## Original article

# Investigation of cellulose nitrate film-based photographic materials (1902–1917) using a portable Raman spectrometer and chemometric methods

Anastasia Povolotckaia<sup>a,b,\*</sup>, Maria Dynnikova<sup>a</sup>, Valeria Lipovskaya (Kaputkina)<sup>a</sup>, Irina Grigorieva<sup>a,c</sup>, Svetlana Kaputkina<sup>a,b</sup>, Evgenii Borisov<sup>a,b</sup>, Anna Vasileva<sup>a,b</sup>, Dmitrii Pankin<sup>b</sup>

<sup>a</sup> State Museum and Exhibition Center ROSPHOTO, 35 Bolshaya Morskaya St., St. Petersburg, 190000, Russia

<sup>b</sup> St Petersburg State University, 7/9 Universitetskaya Emb., St. Petersburg, 199034, Russia

<sup>c</sup> The Stage Hermitage Museum, 190000, St. Petersburg, 34 Dvortsovaya Emb, Russia

## ARTICLE INFO

## Article history:

Received 9 April 2024

Accepted 5 December 2024

## Keywords:

Cellulose nitrate

Raman

PCA

Degradation

Kosse

## ABSTRACT

The study is devoted to the development of a safe and reliable methodology for investigation of photographic stereo negative films by methods of molecular spectroscopy using portable devices. The investigation of 200 photographic stereo negative films of the early XXth century that belonged to the Karl Kosse family photographic archive was performed. This archive was donated to the collection of the State Russian Museum and Exhibition Centre ROSPHOTO (St. Petersburg, Russia) in 2013. Due to the presence of artifacts with a different state of preservation, the study of the artifacts contributes to the understanding of the degradation processes and methods of the state control, approaches of restorations and conservations, as well as the historical development of the photographic industry and amateur photography of the late XIX – early XXth centuries.

The portable Raman spectroscopy was selected as the informative technique, giving highly reproducible results. The film base was attributed to cellulose nitrate with the camphor addition for all studied artifacts. It was demonstrated that the safe and reliable results can be obtained with the help of portable Raman spectrometer BRAVO Bruker. Combination of principle component analysis with conjunction of hierarchical cluster analysis made it possible to divide the studied photographic materials into groups on the basis of relative contribution of inorganic compounds detected by Raman spectroscopy.

© 2024 Elsevier Masson SAS. All rights are reserved, including those for text and data mining, AI training, and similar technologies.

## 1. Introduction

Karl Kosse (1851–1936, St. Petersburg, Russia) was a successful military veterinary, wealthy public official and a classic representative of the amateur photographer of the early XXth century. The images in the photographic collection are inextricably related to the history of the family of Karl Kosse and depict family members, relatives and landscapes. The archive of negative and positive photographic materials created in 1902–1917 years by Karl Kosse arouse great interest from a historical perspective of photography

development as popular art. The artistic value of the archive is determined by careful framing of stereo photographs performed with close adherence to conventional theory of perspective construction in three-dimensional stereo images. The archive originally belonged to Kosse family, and in 2013 it was donated to the State Museum and Exhibition Center ROSPHOTO (St. Petersburg, Russia).

The collection under investigation is a unique example of early film-based photographic materials [1–3]. To avoid their destruction, such objects require special storage conditions (relative low temperatures), and, like all museum collections, could only be examined directly in the museum. Owing to its non-destructive and non-invasive approach as well as high sensitivity, the optical methods are promising for the study of valuable museum objects.

Nowadays, the determination of cellulose nitrate base preservation state is performed by optical methods including methods of vibrational spectroscopy, specifically by Raman spectroscopy [3–6], IR spectroscopy [5–12] and, much less often, by such op-

\* Corresponding author.

E-mail addresses: [anastasia.povolotckaia@spbu.ru](mailto:anastasia.povolotckaia@spbu.ru) (A. Povolotckaia), [editor@rosphoto.org](mailto:editor@rosphoto.org), [gazetamansarde@inbox.ru](mailto:gazetamansarde@inbox.ru) (M. Dynnikova), [himlab@rosphoto.org](mailto:himlab@rosphoto.org) (V. Lipovskaya (Kaputkina)), [irinagrigoireva@mail.ru](mailto:irinagrigoireva@mail.ru) (I. Grigorieva), [svetlana.kaputkina@spbu.ru](mailto:svetlana.kaputkina@spbu.ru) (S. Kaputkina), [eugene.borisov@spbu.ru](mailto:eugene.borisov@spbu.ru) (E. Borisov), [a.a.vasileva@spbu.ru](mailto:a.a.vasileva@spbu.ru) (A. Vasileva), [dmitrii.pankin@spbu.ru](mailto:dmitrii.pankin@spbu.ru) (D. Pankin).

tical methods as luminescence spectroscopy [13] and short-wave infrared (SWIR) reflectance [14].

In the current study, the method of Raman spectroscopy was used for investigation of cellulose nitrate base. This method was chosen due to several advantages. First of all, Raman spectroscopy allows studying laminated objects [3,9] without their mechanical destruction. That is why in case of study of polymeric film base, it is more powerful than IR or luminescence spectroscopes. For example, for infrared (IR) measurements it might be necessary to remove other layers to study the polymeric base [9] which is unacceptable to gelatin-containing photographic artifacts. Thus, studies of the object by Raman spectroscopy are more non-destructive than IR spectroscopy or luminescence spectroscopy with UV excitation. Secondly, in application to photographic objects, the methods of vibration spectroscopy are more informative than methods of UV-Vis or luminescence spectroscopy. At the same time, unlike SWIR reflectance spectroscopy where there is the contribution of overtones, in mid-IR and far-IR parts of vibrational spectrum the fundamental vibrations are appeared. The former is more studied and greater correlation structure-spectrum was investigated. Thirdly, Raman spectroscopy may provide more information compared to IR spectroscopy about inorganic compounds including minerals in composition of artifact under study because characteristic vibrational spectra peaks for inorganic compounds appears including in the region of 100 – 650  $\text{cm}^{-1}$  wavenumbers.

It should be noted, that accurate localization of the area of measurement may be realized in case of con-focal mode of measurement [15] which is available using stationary equipment. However, in case of numerous collections which cannot be transported to a laboratory and should be investigated in the place of storage, the application of portable spectrometers is the only one available alternative way. But it should be taken in mind, that technical parameters of portable setups are usually less precise than for stationary equipment (including laser source power, detector sensitivity, spectral resolution, etc.) that is why the approaches of data proceeding applicable in case of measurements on stationary equipment may be not applicable in case of measurements on portable equipment. All this testifies to the need to study the possibility of using the portable Raman spectrometer for composition identification of museum collections.

Nowadays, handheld Raman spectrometer was used to investigate different nitrate cellulose-based volume objects, namely dental prostheses and billiard balls [4,16]. At the best of our knowledge, the thin-film nitrate cellulose-based objects are mainly investigated using stationary equipment [3]. Thus, it is necessary to study thin-film nitrate cellulose-based objects using handheld (portable) Raman spectroscopy.

As a result of the investigation of numerous museum collections it is possible to obtain a big massive of data. Also, due to technical features of handled setups, the obtained data may have relatively high signal/noise ratio. These two factors lead to the need of specific data proceeding which realize maximum possible percentage of variance allowing finding hidden correlations. The principal component analysis approach could be used as a method of data proceeding [17]. Unlike previous works [3], in current study it is suggested to use this method not only for investigation of nitro-cellulose base state but also for detection of additional inclusions and their nature. Thus, the results of the study of loadings in the principal component analysis approach can allow tracking not only changes in the ratio of peaks of one substance (e.g. polymer base), but also the correlation of peaks with each other (e.g., belonging to one substance), drawing a conclusion about the statistical significance of such a correlation.

Taking into account all the listed aspects, the main goal of the current research was the development of the approach to the study of thin-film photographic materials by handheld Raman

spectroscopy and further data analysis using principal component method. To reach the goal of the research and investigate the Karl Kosse collection it is necessary to answer several questions:

- 1) Is the method of handheld Raman spectroscopy applicable to study of thin-film photographic artifacts?
- 2) What type of polymeric base (cellulose nitrate, cellulose acetate or polyester) do these artifacts have?
- 3) Is it possible to determine other compounds in the structures of photographic artifacts using principal component analysis approach?

In this regard, within the framework of this work, the task was set to clarify the stereo negative base, as well as to identify the composition and development of a methodological approach and recommendations for storage of the early XXth century photographic materials.

The stereo negative film base varies in the type of material used - cellulose nitrate, lately cellulose acetate [7,8]. Forming stereo negative, one side of the base (matte) is covered by outer emulsion layer (photoemulsion) - a colloidal mixture of silver microcrystals in gelatin, making a photosensitive layer. Beneath it a sublayer consisting of hardened gelatin is located, inert with respect to all components of the emulsion layer and necessary to ensure good adhesion of the emulsion to the substrate. The opposite (glossy) side is covered with an anti-curl gelatin layer (counterlayer) [3].

It's worth noting that clear cellulose nitrate plastic film was used by photographers and filmmakers from its invention in the 1880s through the 1950s. Preservation of this material is a problem due to its instability and danger, since pure cellulose nitrate is highly flammable at relatively low ambient temperatures [18]. However, research is still ongoing in this direction with the aim of establishing the exact conditions, decompositions and deflagrations temperatures (which can be higher than indicated up to approximately 180 °C) in real samples depending on the ageing method (heat-humidity ageing and UV irradiation) [18], as well as the composition (e.g. presence and percentage of camphor). Consequently, the identification of the polymer film base and other additives are highly necessary in order to separate and safely store film-based photographic materials. Cellulose nitrate is widely represented in library storage, archives and museum photographic collections.

In this article, samples from the ROSPHOTO collection were examined using a portable Raman spectrometer (BRAVO Bruker), which shows great potential for the rapid and non-invasive identification of film base. A total of 200 film-based stereo negatives were selected for the study, which date back to the period between 1903 and 1917 years.

## 2. Research aim

The work is aimed at the study of the possibility of studying stereo negatives using portable Raman spectroscopy, establishing the polymer base, and studying the similarities and differences in the composition of the film-based photographic materials from the early XXth century from the collection of Karl Kosse. The research and justification of practically important spectral features for the artifacts was provided via portable Raman spectroscopy and chemometric analysis methods. Studying of this approach is crucial for huge amounts of data obtained for large collections analysis, leading to the identification of hidden patterns in the composition and process of aging.

## 3. Materials and methods

### 3.1. Materials

The collection under investigation is a unique example of early film-based photographic materials. The archive consists of 588 ex-

hibits, including film-based negatives (242 items) and stereo negatives (201 items) with a single frame size of  $8.0 \times 7.8$  cm. Ink inscriptions were found on the backside of most negatives, including a number of the item, place and year of its creation and, in some cases, an indication of portrayed people.

A statistically significant amount of 200 stereo negatives was selected for the study, which date back to the period between 1903 and 1917 years. The choice of the set of stereo negatives for the collection made during the 15 years was made in order to identify the general trends in spectral data dealt with structure and composition.

Visual examination of the stereo negatives condition, according to the classification given in [3] are levels 1–3. There were 113 stereo negatives corresponding to level 1 and 87 stereo negatives for levels 2 and 3.

### 3.2. Portable sequentially shifted excitation (SSE) Raman spectrometer Bravo

The portable Raman spectrometer BRAVO (Bruker Corporation, Billerica, MA, USA) was used for the Raman spectroscopic investigation of photographic material composition. It is equipped with the SSE (SSE<sup>TM</sup>) technology [19], which in total allows one to obtain spectra in the  $300\text{--}3200\text{ cm}^{-1}$  by combining two spectral regions. The spectra in  $300\text{--}2200\text{ cm}^{-1}$  region were recorded with 830 nm laser diode excitation and the spectra in  $1200\text{--}3200\text{ cm}^{-1}$  with 785 nm laser diode excitation using the DuoLaser<sup>TM</sup> technology [20]. In each region the three spectra are measured with slightly shifted excitation energy. The mathematical algorithm allows to obtain the peaks which shifts simultaneously along with excitation wavelength change (the Raman peaks) and strongly reduce the luminescence contribution, stray light and environmental artifacts in the spectral region [20–23]. In order to reduce the residual luminescence background, the additional baseline correction was performed in OriginPro2021b (OriginLab Co.; Northampton, MA, USA). Spectra were recorded with a 3000 ms acquisition time and 10 repetitions. For all the measurements OPUS 8.5 was used to select the appropriate acquisition parameters in order to perform safe spectra measurements. The laser power was  $<100$  mW with laser spot diameter about 3 mm. The actual resolution was about  $10\text{ cm}^{-1}$ . The device was used for measurements via a tripod and additional mounts which fix the spectrometer position for stable and reproducible spectra. The film-based stereo negatives were placed in a horizontal plane on the table surface.

### 3.3. Data analysis

#### 3.3.1. Principle component analysis (PCA)

The PCA is one of the oldest (about 40 years) and widely used chemometric technique for data analysis in various fields including natural, technical, social, humanitarian and various multidisciplinary sciences [24]. This method is successfully applicable in chemistry, medicine, biology, economics, agronomy and cultural heritage sciences [17,25,26]. In the cultural heritage, this method has been used to analyze various spectral data, such as XRF, FTIR, Raman, NIR reflectance and LIB spectroscopies data [17], analyzing various substances, e.g. glass, metals and metal oxides, organic matters. In general, the PCA is a multivariate technique that allows the implicit dependences identification during high-dimensional data examination. Additionally, this method allows obtaining the new orthogonal coordinates, accumulating most of the information using significantly smaller number of independent variables, i.e. data dimension reduction [17,24]. The main idea of the PCA is to perform transformations to a new basis of mutually orthogonal vectors (the so-called principal component loadings) which are linear combinations of the original basis vectors. In this case, the

selection of PCs is carried out gradually in order to maximize possible data variance. Thus, the PCs are ordered by the percentage of data explained, with the PC1 describing the maximum possible data variance [24,27–29]. In this study, the usage of the PCA to analyze spectra was limited to the  $300\text{--}1800\text{ cm}^{-1}$  fingerprint region. The reason of excluding hydrogen stretching vibrations region is explained in Results and discussion section. Before performing PCA, the spectra were normalized. Data analysis using the principal component method was carried out in the program Principal Component Analysis for Spectroscopy v1.3 which is incorporated in OriginPro2021b software (OriginLab Co.; Northampton, MA, USA).

#### 3.3.2. Hierarchical cluster analysis (HCA)

HCA was carried out in order to analyze the data common features and differences. Ward's method was chosen as the approach that allows making decisions at each step of clusterization procedure [30]. The main idea of this method is the following: at each step of agglomeration the so-called Ward criterion is applied. This criterion consists of joining the two clusters obtained at the previous stage so that the minimum of variance between elements within the new formed cluster is achieved [31]. The first 10 PCs scores were selected as the data in order to perform clusterization procedure. The Euclidean metrics is used to calculate distance between elements. HCA was performed via OriginPro2021b (OriginLab Co.; Northampton, MA, USA).

## 4. Results and discussion

At the first stage the identification of the film base was performed via a portable Raman spectrometer BRAVO (Bruker). This approach is promising during museum objects study directly at the place of their storage, and photographic film-based stereo negatives made by Karl Kosse represents a good example. The typical obtained spectra from film-based photographic materials are shown in Fig. 1. The presence of peaks at  $850$  and  $1283\text{ cm}^{-1}$  attributed to the stretching vibrational modes  $\nu(\text{N-O})$  and  $\nu_s(\text{NO}_2)$  of cellulose nitrate [6,32,33], was noted in all obtained spectra from the 200 studied artifacts. In addition, the spectra showed a stably reproducing peak around  $649\text{ cm}^{-1}$ , assigned to the camphor. It was added to cellulose nitrate to form celluloid [6]. Other bands from the nitrate groups are also observed at  $625$  and  $690\text{ cm}^{-1}$ . Attribution of identified strong to medium intensive peaks of cellulose nitrate is listed in the Table 1.

The identification of cellulose nitrate (and celluloid) agrees with the historical period of its production. The main disadvantage of this material is low temperature inflammation of cellulose nitrate as well as instability with the tendency to gaseous nitric acid formation [3,18]. The former can not only influence the photographic layers near the base but also possibly interact with material in which artifact is kept. The identification of the polymer film base is necessary in order to separate and safely store film-based photographic materials.

**Table 1**  
Main identified Raman bands of cellulose nitrate.

Raman peak frequency, $\text{cm}^{-1}$	Assignment [4,18,19] <sup>1</sup>
1283	$\nu_s(\text{NO}_2)$
851	$\nu(\text{NO})$
748	$w(\text{NO}_2)$
690	$\delta(\text{NO}_2)$
625	$\rho(\text{NO}_2)$
561	complex vibrations in Pyranose

<sup>1</sup> here and after  $\nu$ ,  $\delta$ ,  $\rho$  and  $\omega$  corresponds to the stretching, bending, rocking and wagging vibrations.  $s$  subscript letter corresponds to the symmetric vibrations.

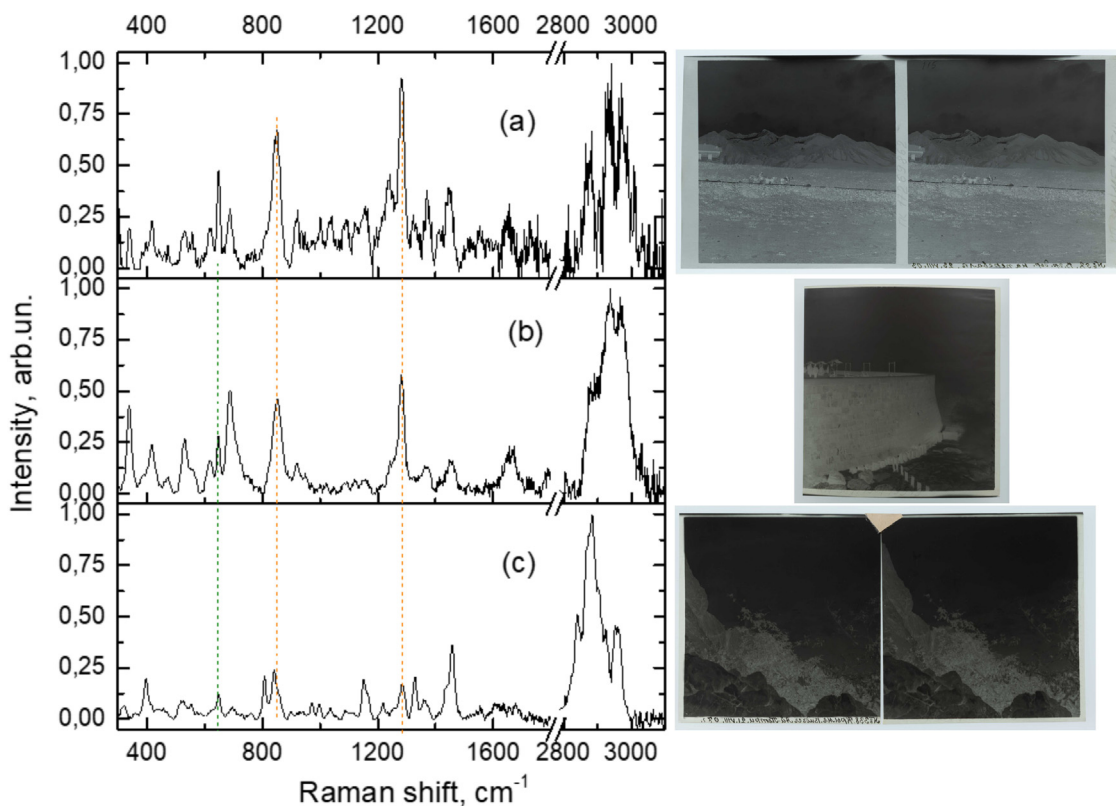


**Fig. 1.** Examples of Raman spectra for the studied samples obtained from photographic materials 381/115 (a), 381/150 (b) and 381/257 (c). The green vertical dotted line highlights the peak  $649\text{ cm}^{-1}$ , orange vertical dashed lines highlight peaks  $851$  and  $1283\text{ cm}^{-1}$ . (For interpretation of the references to colour in this figure legend, the reader is referred to the web version of this article.)

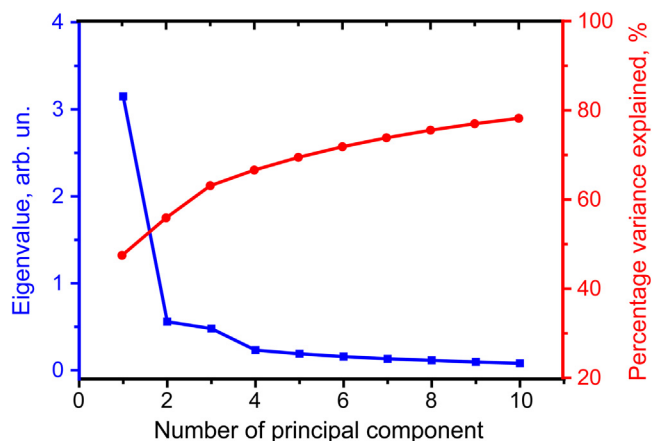


**Fig. 2.** Dependence of the eigenvalue and cumulative percent of explained variance on number of PC.

Once the film base has been determined, the contribution of other substances was studied. In many spectra the normalization by maximum leads to the normalization by  $1283\text{ cm}^{-1}$  peak of cellulose nitrate. The correlated intensity changes in groups of non-polymer peaks was noted for individual photographic stereo negatives.

In order to identify implicit dependencies, the spectra were analyzed using the PCA method. Fig. 2 shows the dependence of the eigenvalues and the percentage of explained variation in the data. The sharp drop when moving from the 3rd to the 4th PC takes place. At the same time, the cumulative percent of explained variance for the first 3 PCs is about 63 %. A cumulative percentage of explained variance and influence of noise in loadings spectra which becomes significantly greater starting with the sixth PC and

to maintain balance between number of components, first 5 PCs were chosen for the following study. With such a cutoff, the eigenvalue for the 6th and subsequent components is  $<10\%$  of the first, and the total percentage of explained variation in the data is about 70 %.

At the next stage, the possibility of grouping the spectra in PCs based on the similarity of the observed spectral features was studied. HCA was chosen as a clustering method with a decision on grouping based on Ward's criterion. The results of cluster analysis are shown in Fig. 3. It can be noted, that as the number of clusters increases, the greatest difference in decision-making distances occurs precisely for the first four clusters. In this regard, it was decided to divide all obtained spectra into four main groups.

Within this approach, the localization of groups in two-dimensional space, which is represented by pairwise combinations of the main components, was noted. The most significant separation of different groups occurred for the case of combinations (PC1, PC2) and (PC2, PC3) shown in Fig. 4. The importance of the first three PCs correlates with their highest eigenvalues and the percentage of data variation they explain, presented in Fig. 2.

In order to understand the physical meaning of the grouping the obtained loadings plot was studied (Fig. 5). As it can be seen for the loading spectrum of PC1, the main weights are in the region up to  $740\text{ cm}^{-1}$ , namely  $338$ ,  $530$  and  $688\text{ cm}^{-1}$ . This region of the Raman spectrum is typical for inorganic oxide substances [34]. Although an exact match couldn't be found, the frequency ranges of the largest weights for the first component are quite close to the regions where the peaks for bending vibrations in  $\text{SiO}_4$  tetrahedra ( $338\text{ cm}^{-1}$ ), bending vibrations in  $\text{SiO}_4\text{-AlO}_4$  ( $530\text{ cm}^{-1}$ ), as well as symmetrical bridging vibrations in  $\text{Si-O}_b\text{-Si}$  ( $688\text{ cm}^{-1}$ ) in various aluminosilicate and/or magnesium aluminosilicate minerals including clay minerals are located [35,36]. Thus, it can be concluded that the spectra of the 4th group in Fig. 4 show the high-

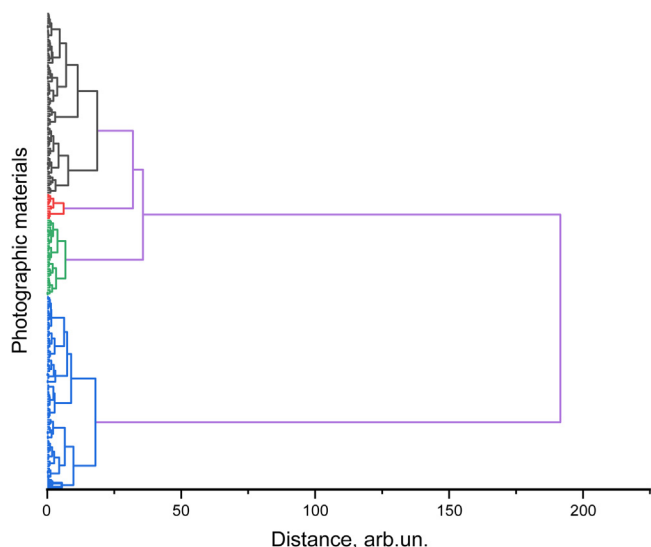


**Fig. 3.** The dendrogram obtained by HCA. The 1st, 2nd, 3rd and 4th groups have black, red, green and blue colors correspondingly (here and after). (For interpretation of the references to colour in this figure legend, the reader is referred to the web version of this article.)

est relative content of the mineral component. As an example of relatively high mineral component contribution the spectrum in Fig. 1b is presented. At the same time this component is much less for groups 1 and 2 (Fig. 1a,c), for group 3 intermediate values are noted. Aluminosilicates could appear in the composition of cellulose nitrate films at the moment of the gelatin layer hardening.

Considering the second and third PCs, the significant weights are much more delocalized and are located in the spectral range typical for organic compounds. So, for PC2, the greatest weight is at  $1460\text{ cm}^{-1}$  located in the region of bending vibrations in  $\text{CH}_2$  groups [32,37,38] (Fig. 5b). For PC3, one of the significant weights was in the region of stretching vibrations  $\nu\text{NO}$  of cellulose nitrate ( $856\text{ cm}^{-1}$ ), and the second one ( $1676\text{ cm}^{-1}$ ) is in the region typical for antisymmetric stretching vibrations in  $\text{NO}_2$  group [33]. Another hypothesis could be linked with stretching vibrations in  $\text{C}=\text{O}$  bond ( $\nu(\text{C}=\text{O})$ ) in the protein based media [32,37,38] which may originate from outer gelatin layers (Fig. 5c). However, it is worth mentioning that the  $\nu(\text{C}=\text{O})$  in degraded cellulose nitrate has higher frequency  $1700\text{--}1730\text{ cm}^{-1}$  [33]. The correlated changes of  $856$  and  $1676\text{ cm}^{-1}$  weights allows supposing the relation with nitrate group. Greater contribution of antisymmetric vibration when normalized by  $1286\text{ cm}^{-1}$  ( $\nu_s(\text{NO}_2)$ ) could be a sign of cellulose nitrate degradation.

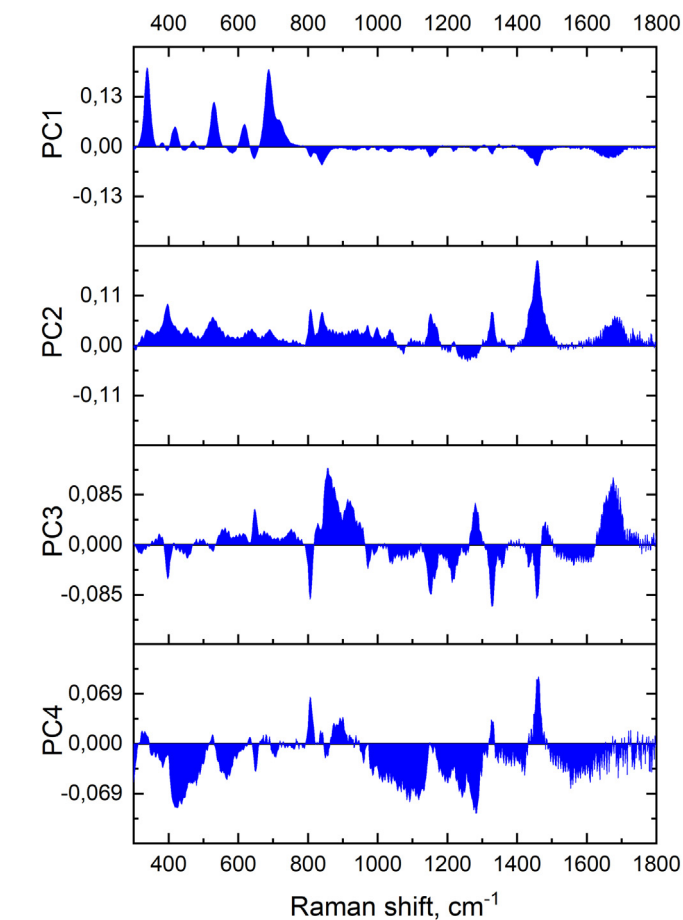
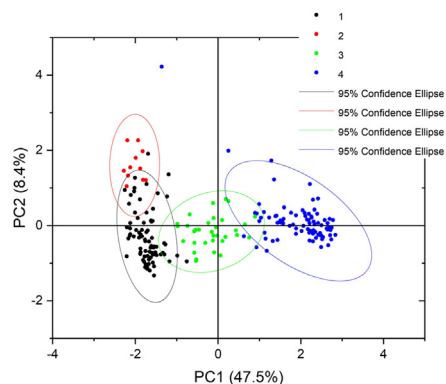


**Fig. 5.** Loadings for the first 4 PCs: PC1(a), PC2(b), PC3(c), PC4(d).

At the same time, for PC2 correlated with the peak at  $1460\text{ cm}^{-1}$ , and for PC3 anticorrelated with the peaks at  $852$  and  $1676\text{ cm}^{-1}$ , the presence of a set of smaller weights (positively and negatively defined peaks in the spectrum) with similar frequencies was noted (Fig. 6a,b). These weights are in good agreement with the most intense peaks of the polypropylene (Fig. 6c), namely  $397$ ;  $809$  and  $838$ ;  $974$ ;  $1151$ ;  $1328$ ;  $1461\text{ cm}^{-1}$ . These maxima are assigned to bending vibrations in CCC ( $397\text{ cm}^{-1}$ );  $\rho(\text{CH}_2)$ ,  $\nu(\text{CC}_b)$ ,  $\nu(\text{C}-\text{CH}_3)$  ( $808\text{ cm}^{-1}$ );  $\rho(\text{CH}_2)$ ,  $\nu(\text{CC}_b)$ ,  $\nu(\text{C}-\text{CH}_3)$ ,  $\rho(\text{CH}_3)$  ( $841\text{ cm}^{-1}$ );  $\rho(\text{CH}_3)$ ,  $\nu(\text{CC}_b)$  ( $974\text{ cm}^{-1}$ );  $\nu(\text{CC}_b)$ ,  $\nu(\text{CCH}_3)$ ,  $\delta(\text{CH})$ ,  $\rho(\text{CH}_3)$  ( $1151\text{ cm}^{-1}$ );  $\delta(\text{CH})$ ,  $\tau(\text{CH}_2)$  ( $1329\text{ cm}^{-1}$ );  $\delta_{\text{asym}}(\text{CH}_3)$ ,  $\delta(\text{CH}_2)$  ( $1461\text{ cm}^{-1}$ ) where  $\nu$ ,  $\delta$ ,  $\rho$  and  $\tau$  correspond to the stretching, bend-

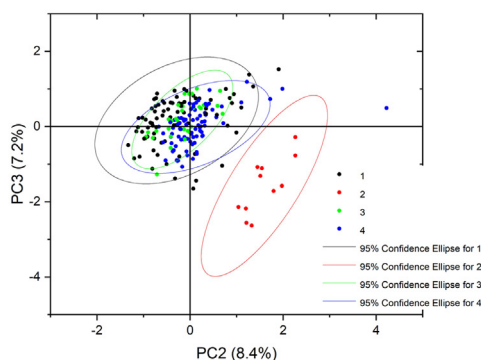


**Fig. 4.** Scores in (PC1,PC2) (a) and (PC2,PC3) (b) coordinates. The 1st, 2nd, 3rd and 4th groups have black, red, green and blue colors correspondingly. (For interpretation of the references to colour in this figure legend, the reader is referred to the web version of this article.)

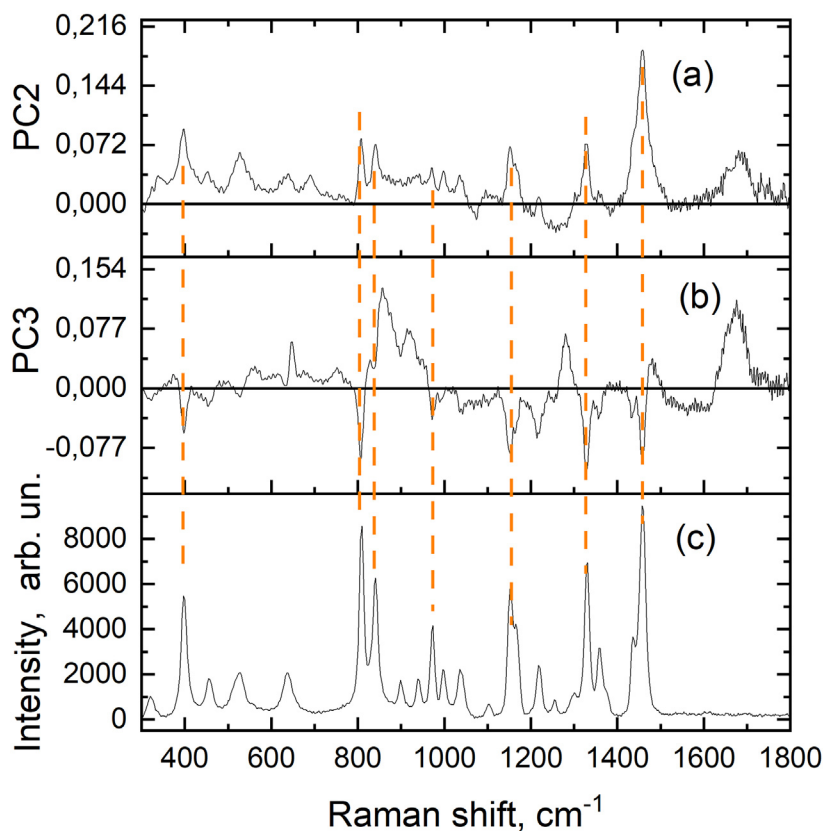


Fig. 6. Loading graphs for PC2 (a) and PC3 (b), and the reference polypropylene spectrum (c).

ing, rocking and twisting vibrations (*asym* subscript corresponds to the antisymmetric vibrations) [39–41].

Thus, a group of film-based photographic materials was identified, which spectra contain a contribution from a fairly modern polymer – polypropylene (Figure S1). It was invented in the early 1950s [42], much later than the dated period of the stereo negatives. The appearance of this polymer may be associated with the storage conditions of photographic stereo negatives, as well as with the release of nitric acid, leading to possible destruction of the packaging in which the stereo negatives are stored. The top gelatin layer also becomes tacky and/or softens over time.

The PC4 is characterized by the presence of broad bands where the highest weights are achieved, for example, 400–460, 1086–1140, 1246 and 1282  $\text{cm}^{-1}$ , along with anticorrelating localized weights at 806 and 1460  $\text{cm}^{-1}$ . In terms of frequency, the given spectral ranges are typical for the cellulose base of the polymer and cellulose derivatives [6,38,43–46]. The following attribution takes place: 400–460  $\text{cm}^{-1}$  ( $\delta(\text{CCC})$ ,  $\delta(\text{OCC})$ ,  $\delta(\text{COC})$  and  $\delta(\text{OCO})$  vibrations in ring), 1086–1140  $\text{cm}^{-1}$  (stretching vibrations in glycosidic COC), and 1246  $\text{cm}^{-1}$  (various bending vibrations with hydrogen  $\delta(\text{COH})$ ,  $\delta(\text{HOC})$ ,  $\delta(\text{HCC})$ ). To sum up, it is possible that PC4 is related to the condition of the substrate of the film-based photographic stereo negatives. The appearance of wider bands may indicate a greater degree of structural disorder in the material. On the other hand, a smaller manifestation of a given PC for spectra normalized to the maximum may indicate a smaller relative contribution from the base.

It should be noted that the greatest extent of the 95 % probability ellipsoid (variability of data) occurs precisely for the second group. In addition, almost all film-based photographic materials from the 2nd group have a positive projection value on PC4 (Figure S2), which indicates a significant contribution to the spec-

trum from polypropylene. The presence of a polypropylene is a clear marker indicating a high degree of degradation of cellulose nitrate, resulting in top gelatin layer softening and  $\text{HNO}_3$  release, group 2 should be separated and isolated.

## 5. Conclusion

In order to preserve and monitor the condition of museum objects, it is extremely important to develop non-destructive and non-contact methods for studying their structure using portable instruments. The example of such technique is Raman spectroscopy using a portable spectrometer. As a part of such investigation, the composition of photographic materials in this article was studied by Raman spectroscopy using handheld Raman spectrometer Bravo (Bruker). The 200 photographic stereo negatives were selected from the collection of the photographic archive of the Kosse family as research objects, located in the collection of the State Museum and Exhibition Center ROSPHOTO (St. Petersburg, Russia).

The portable Raman spectroscopy allowed the identification of polymer base even for relatively thin films of stereo negatives as compared to bulk cellulose nitrate-based materials artefacts investigated earlier by other authors. Thus, the portable Raman spectroscopy could be recommended for further polymer base investigation in similar artifacts. The gelatin layers have no significant contribution in obtained Raman spectra. It was found that all the studied stereo negatives have a cellulose nitrate base, identified by peaks at 850 and 1283  $\text{cm}^{-1}$ , and there is also a camphor additive, identified by a peak at 649  $\text{cm}^{-1}$ . The possibility of safe identification of cellulose nitrate using this approach has been demonstrated.

The application of chemometric analysis methods to the 200 studied spectra from stereo negatives made it possible to divide

the spectra into 4 groups. The division is interpreted based on the largest weights in the loading graphs.

Applying this approach, a variable amount of an inorganic component, presumably originating from an aluminosilicate compound with the most intense peaks in the Raman spectra localized in the region below  $740\text{ cm}^{-1}$ , was found. Based on this criterion, photographs were divided according to the degree of inorganic component content into a group with the highest (4th group), the lowest (1st and 2nd groups) and intermediate (3rd group) amount.

Greater contribution of antisymmetric vibration  $1676\text{ cm}^{-1}$  could be the sign of cellulose nitrate degradation.

The study of PC2 and PC3 made it possible to identify a group of materials that contain peaks in their spectra from a modern type of industrial plastic - polypropylene. Its appearance is a sign of contamination of the photographic stereo negative surface as a result of either short-term or gradual softening and interaction of the upper layer of the stereo negative with the storage material. It is known that polypropylene is a chemically resistant material, but it interacts with  $\text{HNO}_3$ . Thus, the importance of periodic monitoring of the top layer condition in the cellulose nitrate film-based stereo negatives, which are prone to degradation, was shown.

## Acknowledgments

This study was supported by the [Russian Science Foundation](#) (No [24–28–00808](#)). Experimental measurements were performed in Research Laboratory of ROSPHOTO. The authors thank Igor V. Lebedev for fruitful discussions.

## Supplementary materials

Supplementary material associated with this article can be found, in the online version, at [doi:10.1016/j.culher.2024.12.003](https://doi.org/10.1016/j.culher.2024.12.003).

## References

- [1] E. Ciliberto, P. Gemmellaro, V. Iannuso, S. La Delfa, R.G. Urso, E. Viscuso, Characterization and weathering of motion-picture films with support of cellulose nitrate, cellulose acetate and polyester, *Procedia Chem* 8 (2013) 175–184, doi:[10.1016/j.proche.2013.03.023](https://doi.org/10.1016/j.proche.2013.03.023).
- [2] A. Quye, D. Littlejohn, R.A. Pethrick, R.A. Stewart, Investigation of inherent degradation in cellulose nitrate museum artefacts, *Polym Degrad Stab* 96 (2011) 1369–1376, doi:[10.1016/j.polymdegradstab.2011.03.009](https://doi.org/10.1016/j.polymdegradstab.2011.03.009).
- [3] E.A. Carter, B. Swarbrick, T.M. Harrison, L. Ronai, Rapid identification of cellulose nitrate and cellulose acetate film in historic photograph collections, *Herit Sci* 8 (2020) 51, doi:[10.1186/s40494-020-00395-y](https://doi.org/10.1186/s40494-020-00395-y).
- [4] A. Neves, R. Friedel, M.E. Callapez, S.D. Swank, Safeguarding our dentistry heritage: a study of the history and conservation of nineteenth–twentieth century dentures, *Herit Sci* 11 (2023) 142, doi:[10.1186/s40494-023-00989-2](https://doi.org/10.1186/s40494-023-00989-2).
- [5] A. Povolotckaia, S. Kaputkina, I. Grigorjeva, D. Pankin, E. Borisov, A. Vasileva, V. Kaputkina, M. Dynnikova, The nitrate cellulose negatives: degradation study via chemometric methods, *Heritage* 7 (2024) 4712–4724, doi:[10.3390/heritage7090223](https://doi.org/10.3390/heritage7090223).
- [6] A. Neves, E.M. Angelin, É. Roldão, M.J. Melo, New insights into the degradation mechanism of cellulose nitrate in cinematographic films by Raman microscopy, *J Raman Spectros* 50 (2019) 202–212, doi:[10.1002/jrs.5464](https://doi.org/10.1002/jrs.5464).
- [7] J. Bell, P. Nel, B. Stuart, Non-invasive identification of polymers in cultural heritage collections: evaluation, optimisation and application of portable FTIR (ATR and external reflectance) spectroscopy to three-dimensional polymer-based objects, *Herit Sci* 7 (2019) 95, doi:[10.1186/s40494-019-0336-0](https://doi.org/10.1186/s40494-019-0336-0).
- [8] D.Estupiñán Méndez, T. Allscher, Advantages of external reflection and transfection over ATR in the rapid material characterization of negatives and films via FTIR spectroscopy, *Polymers (Basel)* 14 (2022) 808, doi:[10.3390/polym14040808](https://doi.org/10.3390/polym14040808).
- [9] M.V.C. Lozano, G. Scitutto, S. Prati, R. Mazzeo, Deep eutectic solvents: green solvents for the removal of degraded gelatin on cellulose nitrate cinematographic films, *Herit Sci* 10 (2022) 114, doi:[10.1186/s40494-022-00748-9](https://doi.org/10.1186/s40494-022-00748-9).
- [10] N. Jastrzębowska, A. Wawrzyk, N. Uroda, Influence analysis of polyvinyl alcohol on the degradation of artificial leather with cellulose nitrate coating originating from a suitcase stored in the collection of the Auschwitz-Birkenau state museum in Oświęcim, Poland, *Materials* 16 (2023) 7033, doi:[10.3390/ma16217033](https://doi.org/10.3390/ma16217033).
- [11] J.S. Oh, S.R. Lee, M.Y. Hwang, Consolidation and Adhesion of cellulose nitrate of folklore artifacts in the 19–20th century, *J Conserv Sci* 35 (2018) 459–470, doi:[10.12654/JCS.2018.34.6.02](https://doi.org/10.12654/JCS.2018.34.6.02).
- [12] E. Noake, D. Lau, P. Nel, Identification of cellulose nitrate based adhesive repairs in archaeological pottery of the University of Melbourne’s Middle Eastern archaeological pottery collection using portable FTIR-ATR spectroscopy and PCA, *Herit Sci* 5 (2017) 3, doi:[10.1186/s40494-016-0116-z](https://doi.org/10.1186/s40494-016-0116-z).
- [13] A. Neves, M.J. Melo, A.M. Ramos, M.E. Callapez, R. Friedel, M. Réfrégiers, M. Thoury, R. Article, Novel markers to map and quantify degradation on cellulose nitrate-based heritage: at the Submicrometer level using synchrotron UV–visible multispectral luminescence, (2021). <https://doi.org/10.21203/rs.3.rs-505353/v1>.
- [14] E. Catelli, G. Scitutto, S. Prati, M.V. Chavez Lozano, L. Gatti, F. Lugli, S. Silvestrini, S. Benazzi, E. Genorini, R. Mazzeo, A new miniaturised short-wave infrared (SWIR) spectrometer for on-site cultural heritage investigations, *Talanta* 218 (2020) 121112, doi:[10.1016/j.talanta.2020.121112](https://doi.org/10.1016/j.talanta.2020.121112).
- [15] P. Vandenabeele, *Practical Raman spectroscopy – an introduction*, Wiley, Chichester, United Kingdom, 2013, doi:[10.1002/9781119961284](https://doi.org/10.1002/9781119961284).
- [16] A. Neves, R. Friedel, M.J. Melo, M.E. Callapez, E.P. Vicenzi, T. Lam, Best billiard ball in the 19th century: composite materials made of celluloid and bone as substitutes for ivory, *PNAS Nexus* 2 (2023) 1–11, doi:[10.1093/pnasnexus/pgad360](https://doi.org/10.1093/pnasnexus/pgad360).
- [17] J. Riu, B. Giussani, Analytical chemistry meets art: the transformative role of chemometrics in cultural heritage preservation, *Chemometrics and Intelligent Laboratory Systems* 247 (2024) 105095, doi:[10.1016/j.chemolab.2024.105095](https://doi.org/10.1016/j.chemolab.2024.105095).
- [18] V.I. Kepley, M.K. Mahanthappa, Wisconsin Nitrate Film Project White Paper 1 NEH White Paper (December 2015) Project Title: investigation of Cellulose Nitrate Motion Picture Film Chemical Decomposition and Associated Fire Risk, n.d.
- [19] J. Cooper, M. Abdelkader, K. Wise, Method and apparatus for acquiring Raman spectra without background interferences, U.S. Patent No 8570507B1, 2013.
- [20] A. Rousaki, M. Costa, D. Saelens, S. Lycke, A. Sánchez, J. Tuñón, B. Ceprián, P. Amate, M. Montejo, J. Mirão, P. Vandenabeele, A comparative mobile Raman study for the on field analysis of the Mosaico de los Amores of the Cástulo Archaeological Site (Linares, Spain), *J Raman Spectros* 51 (2020) 1913–1923, doi:[10.1002/jrs.5624](https://doi.org/10.1002/jrs.5624).
- [21] M. Vagnini, F. Gabrieli, A. Daveri, D. Sali, Handheld new technology Raman and portable FT-IR spectrometers as complementary tools for the in situ identification of organic materials in modern art, *Spectrochim Acta A Mol Biomol Spectrosc* 176 (2017) 174–182, doi:[10.1016/j.saa.2017.01.006](https://doi.org/10.1016/j.saa.2017.01.006).
- [22] J.B. Cooper, S. Marshall, R. Jones, M. Abdelkader, K.L. Wise, Spatially compressed dual-wavelength excitation Raman spectrometer, *Appl Opt* 53 (2014) 3333, doi:[10.1364/AO.53.003333](https://doi.org/10.1364/AO.53.003333).
- [23] J.B. Cooper, M. Abdelkader, K.L. Wise, Sequentially shifted excitation Raman spectroscopy: novel algorithm and instrumentation for fluorescence-free Raman spectroscopy in spectral space, *Appl Spectrosc* 67 (2013) 973–984, doi:[10.1366/12-06852](https://doi.org/10.1366/12-06852).
- [24] H. Abdi, L.J. Williams, Principal component analysis, *WIREs Computational Statistics* 2 (2010) 433–459, doi:[10.1002/wics.101](https://doi.org/10.1002/wics.101).
- [25] M.J. Smith, A.S. Holmes-Smith, F. Lennard, Development of non-destructive methodology using ATR-FTIR with PCA to differentiate between historical Pacific barkcloth, *J Cult Herit* 39 (2019) 32–41, doi:[10.1016/j.culher.2019.03.006](https://doi.org/10.1016/j.culher.2019.03.006).
- [26] B. Capone, P. Biocca, P. Corsi, C. Meneghini, M. Bicchieri, Does the Artemidorus papyrus have multiple lives? Seeking for the answer in the inks through a Raman and PCA analysis, *J Cult Herit* 48 (2021) 1–10, doi:[10.1016/j.culher.2021.02.003](https://doi.org/10.1016/j.culher.2021.02.003).
- [27] J.E. Jackson, *A User’s guide to principal components*, Wiley, Hoboken, United States of America, 1991, doi:[10.1002/0471725331](https://doi.org/10.1002/0471725331).
- [28] B. Flury, *Common principal components and related models*, Wiley, New York, 1988.
- [29] S. Wold, K. Esbensen, P. Geladi, Principal component analysis, *Chemomet Intell Lab Syst* 2 (1987) 37–52, doi:[10.1016/0169-7439\(87\)80084-9](https://doi.org/10.1016/0169-7439(87)80084-9).
- [30] J.H. Ward Jr., Hierarchical Grouping to Optimize an Objective Function, *J Am Stat Assoc* 58 (1963) 236–244, doi:[10.1080/01621459.1963.10500845](https://doi.org/10.1080/01621459.1963.10500845).
- [31] S. Miyamoto, *Theory of agglomerative hierarchical clustering*, Springer Singapore, Singapore, 2022, doi:[10.1007/978-981-19-0420-2](https://doi.org/10.1007/978-981-19-0420-2).
- [32] D.W. Mayo, F.A. Miller, R.W. Hannah, Course notes on the interpretation of infrared and Raman spectra, 2004.
- [33] D.S. Moore, S.D. McGrane, Comparative infrared and Raman spectroscopy of energetic polymers, *J Mol Struct* 661–662 (2003) 561–566, doi:[10.1016/S0022-2860\(03\)00522-2](https://doi.org/10.1016/S0022-2860(03)00522-2).
- [34] A. Wang, J. Han, L. Guo, J. Yu, P. Zeng, Database of standard Raman spectra of minerals and related inorganic crystals, *Appl. Spectrosc.* 48 (1994) 959–968 <https://opg.optica.org/as/abstract.cfm?URI=as-48-8-959>.
- [35] M. Smirnov, E. Roginskii, A. Savin, A. Oreshonkov, D. Pankin, Density-Functional Study of the Si/SiO<sub>2</sub> Interfaces in Short-Period Superlattices: vibrational States and Raman Spectra, *Photonics* 10 (2023) 902, doi:[10.3390/photonics10080902](https://doi.org/10.3390/photonics10080902).
- [36] J.T. Klopogge, Raman spectroscopy of clay minerals, *Develop. clay Sci* 8 (2017) 150–199, doi:[10.1016/B978-0-08-100355-8.00006-0](https://doi.org/10.1016/B978-0-08-100355-8.00006-0).
- [37] P. Vandenabeele, B. Wehling, L. Moens, H. Edwards, M. De Reu, G. Van Hooydonk, Analysis with micro-Raman spectroscopy of natural organic binding media and varnishes used in art, *Anal Chim Acta* 407 (2000) 261–274, doi:[10.1016/S0003-2670\(99\)00827-2](https://doi.org/10.1016/S0003-2670(99)00827-2).
- [38] D. Pankin, A. Povolotckaia, E. Borisov, S. Rongonen, A. Mikhailova, T. Tkachenko, N. Dovedova, L. Rylkova, A. Kurochkin, Investigation of wafers

- used as paper binding in the academician von Struve manuscripts, *J Cult Herit* 51 (2021) 125–131, doi:[10.1016/j.culher.2021.08.005](https://doi.org/10.1016/j.culher.2021.08.005).
- [39] V. Nava, M.L. Frezzotti, B. Leoni, Raman spectroscopy for the analysis of microplastics in aquatic systems, *Appl Spectrosc* 75 (2021) 1341–1357, doi:[10.1177/00037028211043119](https://doi.org/10.1177/00037028211043119).
- [40] E. Andreassen, Infrared and Raman spectroscopy of polypropylene, *Polypropylene: an AZ* (1999) 320–328, doi:[10.1007/978-94-011-4421-6\\_46](https://doi.org/10.1007/978-94-011-4421-6_46).
- [41] M.C. Tobin, The infrared spectra of polymers. III. the infrared and Raman spectra of isotactic polypropylene <sup>1</sup>, *J Phys Chem* 64 (1960) 216–219, doi:[10.1021/j100831a007](https://doi.org/10.1021/j100831a007).
- [42] I. Baker, Polypropylene, in: *Fifty materials that make the world*, Springer International Publishing, Cham, 2018, pp. 169–173, doi:[10.1007/978-3-319-78766-4\\_32](https://doi.org/10.1007/978-3-319-78766-4_32).
- [43] H.G.M. Edwards, D.W. Farwell, D. Webster, FT Raman microscopy of untreated natural plant fibres, *Spectrochim Acta A Mol Biomol Spectrosc* 53 (1997) 2383–2392, doi:[10.1016/S1386-1425\(97\)00178-9](https://doi.org/10.1016/S1386-1425(97)00178-9).
- [44] K. Zhang, E. Brendler, S. Fischer, FT Raman investigation of sodium cellulose sulfate, *Cellulose* 17 (2010) 427–435, doi:[10.1007/s10570-009-9375-0](https://doi.org/10.1007/s10570-009-9375-0).
- [45] M. de Veij, P. Vandenabeele, T. De Beer, J.P. Remon, L. Moens, Reference database of Raman spectra of pharmaceutical excipients, *J Raman Spectros* 40 (2009) 297–307, doi:[10.1002/jrs.2125](https://doi.org/10.1002/jrs.2125).
- [46] J.H. Wiley, R.H. Atalla, Band assignments in the raman spectra of celluloses, *Carbohydr Res* 160 (1987) 113–129, doi:[10.1016/0008-6215\(87\)80306-3](https://doi.org/10.1016/0008-6215(87)80306-3).